https://doi.org/10.1595/205651324X17048925195038 *Johnson Matthey Technol. Rev.*, 2024, **68**, (4), 593–606

JOHNSON MATTHEY
TECHNOLOGY REVIEW
technology.matthey.com

Synchrotron Infrared Microspectroscopy of Zeolite Catalysts

Studying reactivity in real time

By Russell F. Howe*
University of Aberdeen, AB24 3UE, UK

Paul A. Wright
EastCHEM School of Chemistry, University of St Andrews, KY16 9ST, UK

Ivalina Tuxworth[¶]
EastCHEM School of Chemistry, University of St Andrews, KY16 9ST, UK

Mark D. Frogley
MIRIAM beamline B22, Diamond Light Source, Harwell Science and Innovation Campus, Didcot, OX11 0DE, UK

Gianfelice Cinque
MIRIAM beamline B22, Diamond Light Source, Harwell Science and Innovation Campus, Didcot, OX11 0DE, UK; Multifunctional Material & Composite Lab, Department of Engineering Science, University of Oxford, OX1 3PJ, UK

***Email:** r.howe@abdn.ac.uk

[¶]**Present address**: Johnson Matthey, Billingham, TS23 1JD, UK

PEER REVIEWED

Received 30th September 2023; Revised 10th January 2024; Accepted 10th January 2024; Online 10th January 2024

This article reviews recent work undertaken at the beamline B22 of the Diamond Light Source using infrared (IR) microspectroscopy to characterise zeolite catalysts and to study their reactivity in real time. The advantage of vibrational microspectroscopic analysis when linked to the brightness and spectral bandwidth of synchrotron IR light are illustrated. The high spatial resolution means that the uniformity of acid site concentrations within individual large crystals of zeolites and between different crystals can be readily checked and changes to acid site concentrations within crystals resulting from steam treatment mapped. When an *in situ* reaction cell is coupled with mass spectrometric analysis of evolved gases the rapid time response of the method has provided new insight into the initial stages of the conversion of methanol to hydrocarbons over ZSM-5 and SAPO-34 single crystals. Future prospects for applying the method to other types of zeolite catalysed reactions with improved reaction cell design are also discussed.

Introduction

IR spectroscopy is a widely used technique in the field of zeolite chemistry and catalysis (1). The technique has been used for many years to characterise zeolite catalysts. The advent of fast scanning Fourier transform spectrometers (FTIR) and more recently coupled with sophisticated *in situ* reaction cells has led to so-called *operando* IR spectroscopy, where adsorbed species within a zeolite catalyst can be observed during reaction under conditions approximating those in a catalytic reactor (2–5).

Two methods of sample presentation are typically used: either transmission of the IR beam through pressed disks of zeolite powder, or collection and analysis of IR light diffusely scattered from

the surface of a loose bed of zeolite powder, the so-called diffuse reflectance infrared Fourier transform spectroscopy (DRIFTS) technique. Transmission is the standard method and in principle gives better quality spectra than DRIFTS with fewer artefacts. In practice however the quality of the spectra depends critically on the thickness of the pressed disk, which in turn is dependent on the crystal size and morphology of the zeolite. DRIFTS can be readily applied to loose powders of zeolites, but the quality of spectra can be degraded by contributions to the measured signal from specular reflectance, which can only be overcome by diluting the sample with an inert matrix.

The possibility of using IR microspectroscopy to obtain vibrational spectra from single crystals of zeolite catalysts was first demonstrated using benchtop IR microscopes (6). These authors collected spectra from a 30 × 30 μm^2 area of ZSM-5 zeolite crystals at 2 min intervals during thermal decomposition of the tetrapropylammonium fluoride template used to synthesise the zeolites. Later workers used linearly polarised IR radiation to study the orientation of template molecules, the acid site hydroxyl groups and adsorbed molecules in single crystals of AlPO, SAPO and ZSM-5 zeolites (7–10). Microspectroscopy of large ZSM-5 crystals was also used to show the presence of diffusion barriers at the interfaces between intergrowths of different orientations within large ZSM-5 crystals (11).

In applications using a laboratory FTIR spectrometer, signal to noise limitations restricted the limiting aperture sizes to typically above 20 × 20 μm^2, meaning that the method was limited to relatively large crystals. For the same reason, scan times of 60 s or longer were required, limiting the possibilities of observing rapid changes. These limitations can be overcome in principle by utilising the much brighter IR beam obtained from a synchrotron, typically two orders of magnitude brighter than a laboratory Globar source in the mid IR range. Stavitski *et al*. first showed that synchrotron IR microspectroscopy was able to follow in real time the oligomerisation of styrene in individual crystals of ZSM-5 100 × 20 μm^2 in size. Using an aperture as small as 3 × 3 μm^2 they were able to map the distribution of oligomer product within the crystal (12). Later studies by this group included reactions of thiophene in single crystals of ZSM-5 (13) and reactions of methanol and ethanol in single crystals of SAPO-34 (14, 15).

The present review will focus on IR microspectroscopy performed on the Multimode Infrared Imaging and Microspectroscopy (MIRIAM) beam line (B22) at the Diamond Light Source over the past ten years in the specific field of catalysis applications. This will mostly be a summary of published work, although some hitherto unpublished data will also be included.

Experimental Aspects

The MIRIAM beam line at Diamond is described in detail in reference (16). This is equipped with two Bruker Hyperion 3000 IR microscopes coupled to Bruker Vertex 80V FTIR spectrometers. Zeolite crystals are mounted in a Linkam FTIR600 environmental cell. The cell body was modified and a custom made thin heater was used to reduce the IR path length and volume of the cell and allow the 36× microscope optics to be used as both condenser and objective. The crystals are sprinkled onto a calcium fluoride window within the cell, which is then mounted onto the microscope sample stage operating in transmission mode through upper and lower outer windows.

During catalysis experiments, the Linkam cell is connected to a gas-controlling rig fitted with remote-controlled mass flow controllers and valves which allows gaseous reactants to be injected into a nitrogen carrier gas stream as either short pulses or continuous flow. Liquid reactants are injected into the carrier gas stream by syringe *via* a septum. The outlet gases from the Linkam cell are monitored continuously with a rapid scanning quadrupole mass spectrometer. To achieve sufficient sensitivity for mass spectrometry (MS) analysis, around 0.1 mg of crystals is spread across the sample window in the cell, even if the microspectroscopy analysis is performed on one crystal at a time. To relate the online MS signal to the micro FTIR changes on single crystals, it is important that each crystal in a batch is of similar size, so the synthesis of crystals of appropriate quality and dimensions is an essential enabling step for these studies. **Figure 1** shows a schematic of the experimental set up for catalysis at MIRIAM.

For the published work presented here, crystals were synthesised and calcined at the University of St Andrews and fully characterised by scanning electron microscopy (SEM), energy dispersive X-ray (EDX), X-ray diffraction (XRD), X-ray fluorescence (XRF), thermogravimetric analysis (TGA), elemental analysis, ammonia temperature programmed desorption (TPD), porosimetry, solid state nuclear magnetic resonance (SS-NMR) and microcatalytic testing on a fixed-bed reactor.

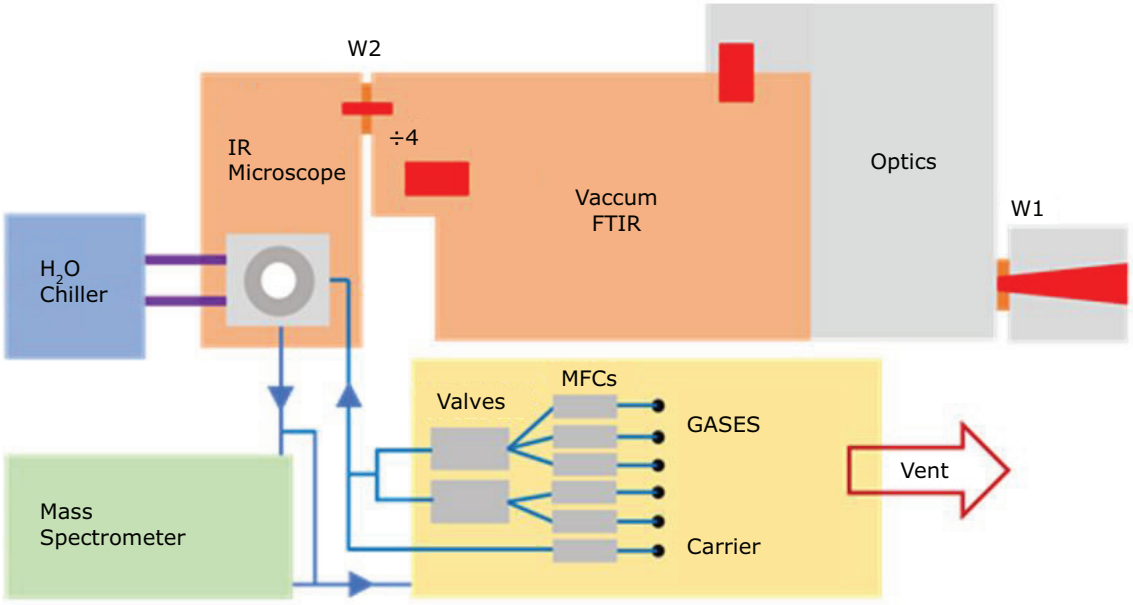

Fig. 1. Schematic of the experimental set up for catalysis studies on zeolite single crystals at the MIRIAM beamline

Characterisation of Zeolites

The ability of IR microspectroscopy to examine individual crystals down to the 10 μm linear scale has allowed detailed vibrational characterisation of zeolite and metal-organic framework (MOF) single crystals. In early studies dehydrated crystals were examined in an unmodified Linkam cell. This allowed crystals to be studied in a flowing nitrogen (or dry air) gas stream as the temperature was raised. Our initial measurements focused on the Brønsted acid sites found in large crystals of HZSM-5, the zeolite which finds wide application in commercial technologies such as catalytic cracking (FCC), xylene isomerisation and methanol to hydrocarbons (methanol to gasoline (MTG), methanol to olefins (MTO) and Mobil's olefin-to-gasoline/distillate). It is possible to grow crystals of ZSM-5 as large as 500 × 200 μm, but an important question with such large crystals is the extent to which the Brønsted acid sites associated with the catalytic activity are uniformly distributed through the crystal. Brønsted acid sites are found when Al^{3+} is substituted for Si^{4+} in any silicate lattice and can be represented as Si(OH)Al, i.e. a hydroxyl group bridging between silicon and aluminium.

Figure 2 shows a set of FTIR microspectra measured across the width of a 120 μm wide HZSM-5 crystal. The transmitted IR beam was collected through a 5 × 20 μm^2 aperture and spectra recorded of a series of overlapping 5 × 20 μm^2 slices across the crystal. In these early experiments it was difficult to achieve and maintain the zeolite in a fully dehydrated state. The spectra in **Figure 2** are dominated by the intense narrow band at 3600 cm^{-1} which is the ν(OH) mode of the Brønsted acid sites, but a weaker series of four bands can also be seen which are characteristic of single water molecules hydrogen-bonded to Brønsted acid sites (17). The bands below 2000 cm^{-1} are due to overtones and combinations of the intense stretching modes of the aluminosilicate lattice, which are of course particularly intense in these large (~100 μm thick) crystals. The overtone bands are however useful for normalising spectra from crystals of differing thickness.

What this early data shows is that the Brønsted acid sites are uniformly distributed across the crystal (as is the residual adsorbed water). The IR microbeam passes through the entire thickness of the crystal but will sample a greater proportion of the near surface regions at the edges and these regions have similar acid site populations to the bulk.

The spatial resolution achievable in light and IR microscopy is constrained by optical diffraction, which manifests when the aperture size becomes comparable with the wavelength of the IR radiation (2–20 μm for the mid IR region). Spectroscopically, high quality spectra (measured as high signal to

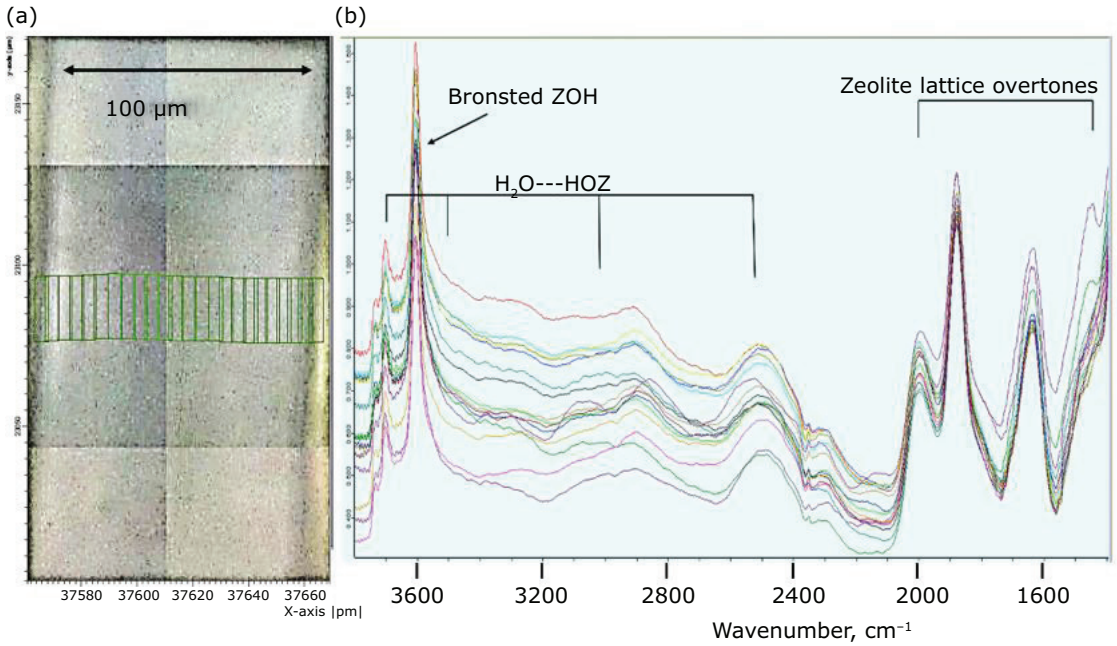

Fig. 2. (a) Optical image of a partially dehydrated large H-ZSM-5 crystal showing the locations of the overlapping slices marked with green boxes; (b) IR microspectra of a series of 5 × 20 µm slices across the width of the crystal (spectra displaced vertically to reduce overlap)

noise ratio) require the sample thickness to be in a range for which the absorption is sufficiently intense to be detected and within the dynamic range of the mercury cadmium telluride (MCT) detector (ideally absorption bands from 0.01 to several absorbance units).

Notwithstanding the much greater brightness (photon flux density) of the synchrotron source compared with a laboratory Globar®, both parameters of slit size and crystal dimension need to be optimised for the sake of spatial resolution and spectral quality, or equivalently throughput in terms of acquisition time. In practice, we have found that for zeolites, crystal sizes of at least 20 µm are necessary to be able to measure spectra within a few seconds of FTIR spectroscopy. It is possible to examine multiple crystals quickly to check the homogeneity of the zeolite sample, which is an important advantage of microsampling.

Figure 3 shows as an example a selection of spectra in the ν(OH) region of three different sizes of dehydrated H-ZSM-5 crystals (note that these crystals are completely free of residual adsorbed water with the improved gas handling rig employed). All three contained similar concentrations of Brønsted acid sites as determined by bulk analysis (Si:Al~30) (18). The differences in intensities of the ν(OH) band between the three sets of spectra are due to the different thicknesses of the crystals. Within each set of crystals, however the ν(OH) bands are remarkably similar regardless of which particular crystal is measured or how it was oriented in the microscope, confirming the homogeneity of the samples. Also visible in the spectra are weak bands at around 3740 cm^{-1}, which are present in all crystals. These bands are usually assigned to SiOH groups terminating the crystal lattice at the external surfaces of zeolite crystals. While this may be the case for microcrystalline samples analysed by conventional (macro-sampling) FTIR, the contribution of surface groups to the transmission spectra of the single crystals measured here will be negligible. The alternative explanation is that the SiOH groups are present at the interfaces between intergrowths within the crystals. Micrometre-resolved XRD imaging of large ZSM-5 crystals has revealed that such crystals contain intergrowths of two different orientations of the zeolite lattice in which the a and b axes are interchanged (19). The boundaries between such intergrowths are likely to contain SiOH groups terminating each sub-lattice.

SAPO-34 is a zeolitic material based on a microporous aluminophosphate lattice in which replacement of P(V) by Si(IV) produces a negative charge which is balanced by a proton behaving as a Brønsted acid, formally Al(OH)SiOAl. HSAPO-34 is used as a commercial catalyst in the MTO process. We have used the MIRIAM IR microscope to

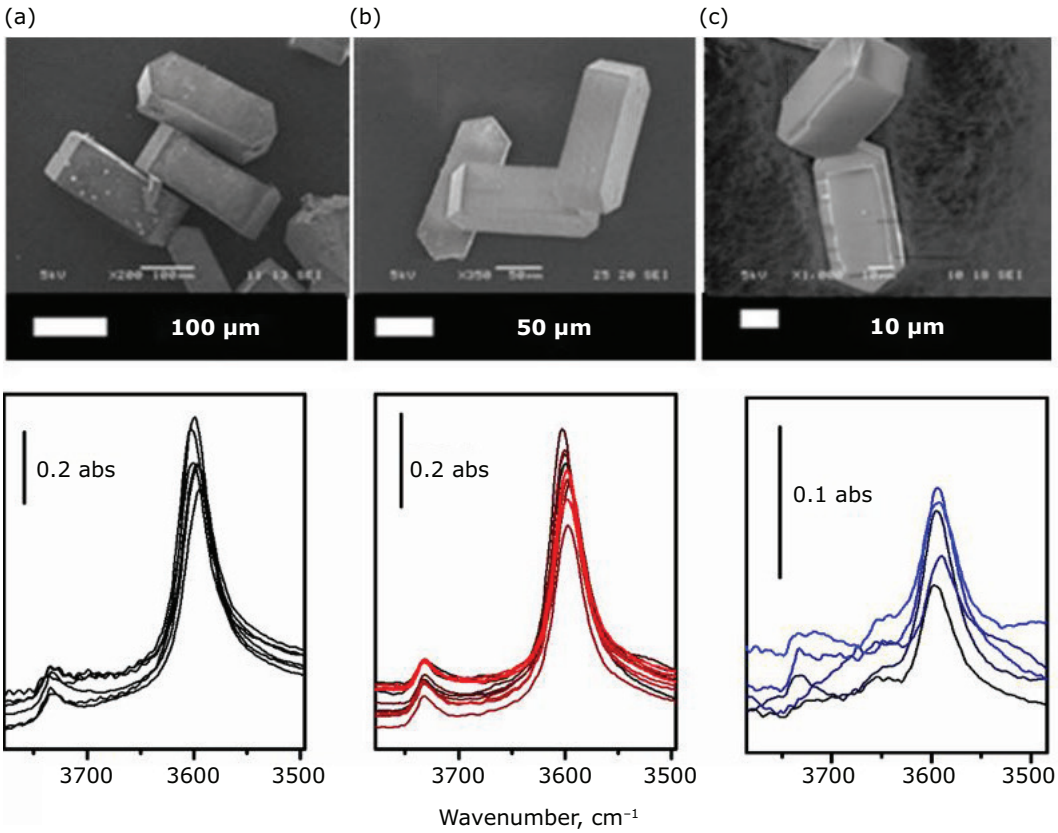

Fig. 3. SEM images and IR microspectra in the hydroxide stetching region of three batches of different sized ZSM-5 crystals containing Si:Al ratios of ~30. SEM images show the crystal sizes: (a) 100 µm; (b) 50 µm; (c) 10 µm. Reproduced from (18) with permission from Royal Society of Chemistry

characterise and map the Brønsted acid hydroxyl groups in single crystals of HSAPO-34. **Figure 4** shows that these crystals contain two types of hydroxyl group populating different sites within the crystal lattice. Mapping the intensity of the ν(OH) bands across the crystal shows that the Brønsted sites are uniformly distributed within the crystal and spectra measured from different crystals confirming the homogeneity of the sample.

Catalytic Chemistry: Methanol to Hydrocarbons

As described in the Experimental section, in later developments the MIRIAM beam line was equipped with a customised Linkam FTIR600 cell in the Hyperion 3000 IR microscope used as an *in situ* catalytic reactor. We have applied this capability extensively to study the conversion of methanol and dimethyl ether over single crystals of H-ZSM-5 (so-called MTG chemistry) and HSAPO-34 (MTO chemistry) (18, 20, 21).

The mechanism of formation of the first carbon-to-carbon bonds from oxygen containing precursors methanol and dimethylether has been puzzled over ever since the first announcements of methanol to hydrocarbon catalysis almost 50 years ago (22). Many different mechanistic schemes have been proposed, with varying degrees of experimental support. Early IR and NMR measurements showed the formation of surface methoxy groups through reaction of methanol or dimethylether with Brønsted acid hydroxyl groups and there is general agreement that light alkenes (ethene and propene) are the first carbon-to-carbon bonded products to appear. This reaction sequence (methanol → methoxy groups → alkenes) is seen very clearly in the IR microspectroscopy experiment illustrated in **Figure 5**.

Injection of a pulse of methanol into a crystal of HZSM-5 held at 573 K causes the immediate loss of the ν(OH) band in **Figure 5(a)**. Most of this intensity loss over the first 50 s is due to the formation of surface methoxy groups, with a smaller contribution from hydrogen bonding to methanol and to dimethyl ether which is formed within a few seconds, as can be seen in the MS analysis of the effluent gases in **Figure 5(b)**. The IR spectrum initially (<60 s) shows the presence of hydrogen-bonded methanol and

dimethylether superimposed on the ν(CH) signature of surface methoxy groups, a characteristic pair of bands at 2980 cm^{-1} and 2870 cm^{-1}.

Subsequently, there is a small recovery of ν(OH) intensity for ~150 s following injection of methanol due to desorption of the hydrogen bonded methanol and dimethylether, leaving the surface methoxy groups unchanged. After 186 s in this particular experiment there is a sudden dramatic recovery of ~90% of the original ν(OH) intensity. At the same time the MS analysis shows the sudden evolution of propene (m/z = 41) and butene (m/z = 55). The earlier m/z = 41 signal is due to fragmentation of dimethylether. Simultaneously the ν(CH) pattern of surface methoxy groups is converted within several seconds to a new pattern identical to that seen if propene is injected into a crystal of H-ZSM-5 and assigned to surface alkoxide species (the green spectrum in **Figure 5(c)**).

This induction period in alkene formation correlating with recovery of hydroxyl groups and conversion of surface methoxy groups to alkoxide species was found to be completely reproducible for crystals of similar sizes, although the induction time was shorter in smaller crystals (18).

When the same experiment was carried out using methanol-d_3 the formation of (partially deuterated) alkenes after an induction period coincided with the breaking of C–D bonds in the surface methoxy-d_3

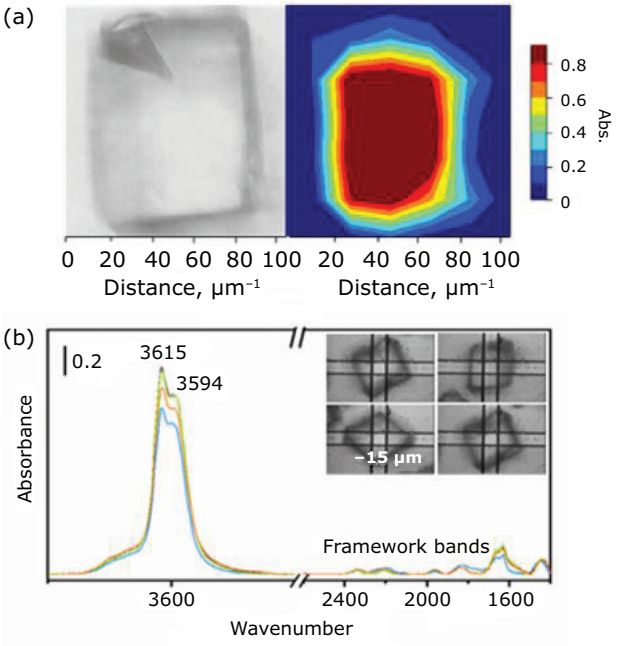

Fig. 4. (a) Optical image and distribution of Brønsted acid sites within one HSAPO-34 crystal, integrated hydroxide intensity between 3650 cm^{-1} and 3550 cm^{-1} and peak normalised to 1; (b) FTIR microspectra of four individual dehydrated HSAPO-34 crystals of similar size (inset), measured with a 15 × 15 $μm^2$ aperture. Note that the exact frequencies are temperature dependent; the spectra shown were measured at 623 K. Reprinted from (21) under Creative Commons attribution License 4.0 (CC-BY-NC 4.0)

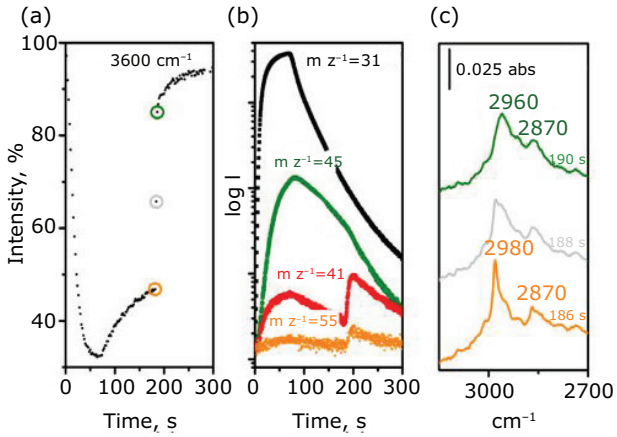

Fig. 5. (a) Absorbance intensity of OH band of a ZSM-5 crystal at 573 K following injection of a pulse of methanol; (b) MS analysis of the effluent gas from the cell following injection of the methanol; (c) spectra in the CH stretching region between 186 s and 190 s after injection. Reprinted with permission from (20), 2019, American Chemical Society

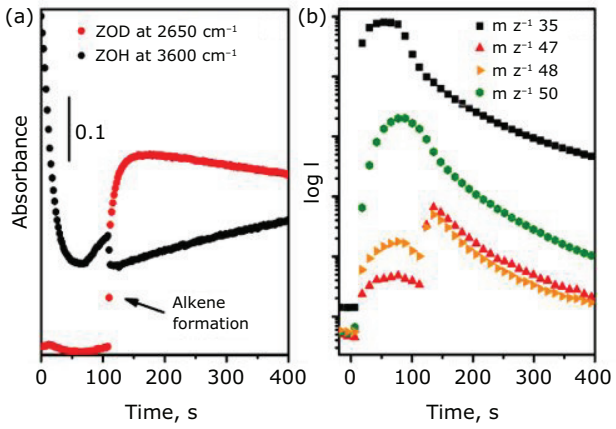

Fig. 6. (a) Intensities of ν(OH) and ν(OD) bands following injection of 8 μl CD_3OH over a ZSM-5 crystal at 573 K; (b) MS analysis of evolved gases. m/z = 35 measures CD_3OH, m/z = 50 measures CD_3OCD_3, m/z = 48 measures propene-d_6 (with a contribution from fragmentation of CD_3OCD_3), m/z = 47 measures propene-d_5. Reprinted with permission from (20), 2019, American Chemical Society

groups, generating ν(OD) bands, as shown in **Figure 6**.

These IR microspectroscopy experiments confirm the importance of surface methoxy groups in generating the first alkenes to be formed from methanol or dimethylether in ZSM-5. The correlation between breaking of the C–H bonds in the surface methoxy groups and the first appearance of alkenes suggests strongly that surface carbene-like species (CH_2) play a key role in the initial alkene formation. We have proposed from these experiments and similar studies on HSAPO-34 single crystals (21) that the induction period results from the initiation of an autocatalytic sequence in which an initial ethene, formed from an ethoxide species generated by carbene insertion from one methoxy group into another, then propagates the carbon-carbon bond forming reaction throughout the crystal through facile diffusion and methylation of the ethene by further surface methoxy groups, as illustrated in **Scheme I**.

IR microspectroscopy is able to observe these events in real time when methanol or dimethylether first enters an individual crystal of the catalyst at reaction temperature. Conventional macro-sampling FTIR spectroscopy cannot achieve this degree of time resolution when not all crystals in the sample see the entry of methanol at exactly the same time.

Once the first alkenes are formed, subsequent chemistry involves oligomerisation of alkenes to form longer chain alkoxide species, which may crack to form alkenes or cyclise to form the so-called hydrocarbon pool within the zeolite pores which is the key to steady state product formation in MTG and MTO catalysis (22). Formation of the hydrocarbon pool and gasoline products under steady state conditions can also be seen in the FTIR microspectroscopy experiments with ZSM-5 crystals. **Figure 7** shows for example spectra recorded during exposure of a crystal of H-ZSM-5 to a continuous flow of dimethyl ether at 623 K,

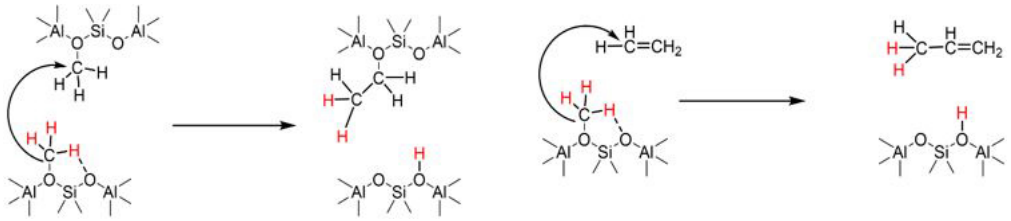

Scheme I. Concerted dissociation of surface methoxy group and carbene insertion into adjacent surface methoxy group to form a surface ethoxide species and liberate a hydroxyl group, followed by elimination of ethene from the ethoxide and propagation of C–C bond forming reaction through carbene-like insertion into C–H bond of ethene. Reprinted from (21) under Creative Commons attribution License 4.0 (CC-BY-NC 4.0)

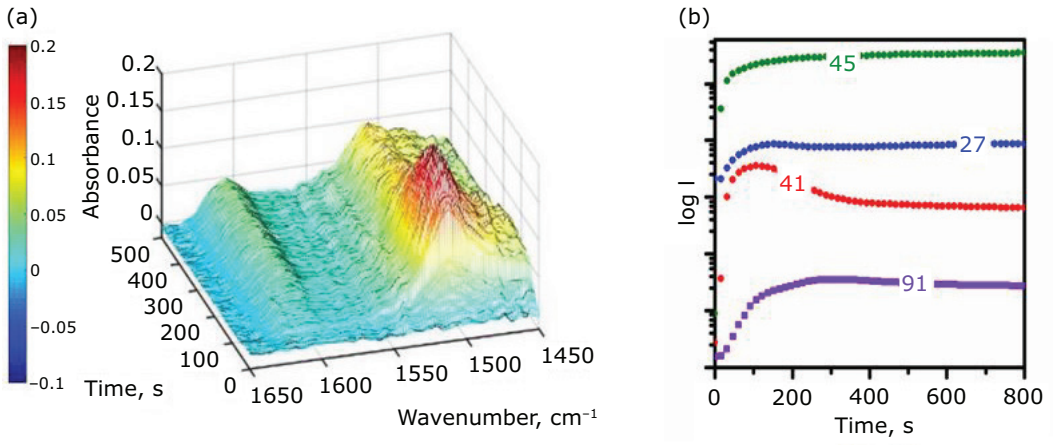

Fig. 7. (a) IR spectra recorded at 2 s intervals during exposure of a ZSM-5 crystal (160 × 60 × 60 μm^3) to a continuous flow of dimethyl ether at 623 K; (b) the MS analyses of the effluent from the reaction cell: m/z = 45 measures dimethyl ether, m/z = 27 is due to fragmentation of dimethyl ether with a possible contribution from ethene, m/z = 41 is due to propene and fragmentation of dimethyl ether, m/z = 91 measures methyl aromatic products. Reproduced from (18) with permission from Royal Society of Chemistry

together with the on-stream MS analysis of gas phase products. The intense band appearing rapidly at 1510 cm^{-1} is due to methyl cyclopentenyl species generated by cyclisation of alkoxide species formed from alkenes. The growth of these species in the early stages of the reaction correlates with the appearance of an m/z = 41 signal in the MS due to propene (superimposed on a baseline signal due to fragmentation of dimethyl ether). As the 1510 cm^{-1} band and the propene MS signal decline, a new IR band grows at ~1620 cm^{-1} which is characteristic of adsorbed aromatic molecules and this correlates with the appearance of an MS signal at m/z = 91 which is due to the tropylium ion formed as a fragmentation product in the MS typical of methyl aromatic molecules.

Catalytic Chemistry: Steam Treatment of HSAPO-34 Enhances Lifetime in the MTO Reaction

IR microspectroscopy at the MIRIAM beam line has provided new insight into the effects of steam treatment on the structure of the HSAPO-34 zeolite catalyst used for the production of light alkenes from methanol or dimethyl ether (MTO and DMTO). The MTO and DMTO technologies have become important worldwide because of their potential to produce alkene feedstocks from coal, natural gas or biomass (23). During operation the cages within the HSAPO-34 structure become filled with polyaromatic molecules and access of reactants to the Brønsted acid sites becomes blocked. Continuous running of the process is only possible *via* fluidised bed technology and associated continual regeneration of the deactivated catalyst, which can be carried out in steam and at elevated temperatures (24, 25).

Hydrothermal treatment of HSAPO-34 at temperatures up to 973 K causes significant loss of acidity associated with silicon redistribution within the framework while retaining the microporosity and the crystal structure of the catalyst. Such moderate exposure to steam can in fact prolong the catalyst lifetime in laboratory fixed bed reactor tests, whereas steam treatment above 973 K causes irreversible loss of porosity and catalytic activity (26).

A complex silicon redistribution occurs when HSAPO-34 is exposed to steam at 923 K, a core-shell structure becomes well developed, visible by optical or SEM, in the core of which there is loss of structure, densification and the development of mesopores. Similar effects are seen in a commercial, microcrystalline powder and in large single crystals and the single crystals of HSAPO-34 are amenable to synchrotron IR microspectroscopy. The microspectroscopic method was applied to map the acid sites across a large HSAPO-34 crystal after moderate exposure to steam to gain insight into the complex silicon redistribution in framework acid sites within the core-shell structure (**Figure 8**).

In the dehydrated, calcined form, the hydroxyl groups are uniformly distributed throughout the crystal, as seen by mapping the intensity of the hydroxyl bands (**Figure 8(a)**). Steaming at 923 K for 20 h reduces the number of acid sites uniformly throughout the crystal (**Figure 8(b)**). After

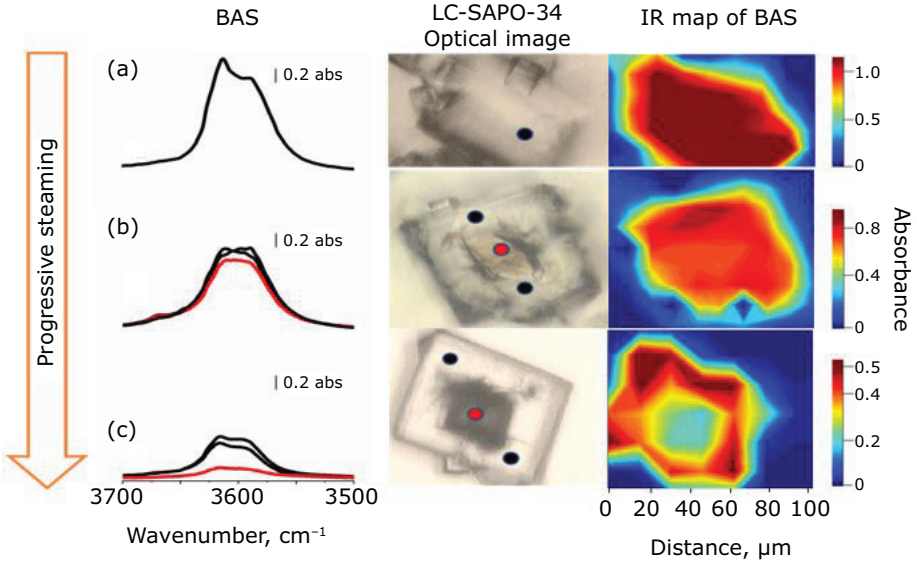

Fig. 8. FTIR microspectra collected in transmission over the crystal edge (in black) and middle (in red) revealing the dark patches seen in optical micrographs have lost Brønsted acid sites (BAS). Map of the 3600 cm^{-1} hydroxyl band intensity across crystal: (a) calcined; (b) steamed 923 K 20 h; (c) steamed 973 K 20 h. Reprinted from (26) with permission from Elsevier

steaming at 973 K for 20 h however, the optical image of the crystal shows clearly the development of a core-shell structure with the centre of the crystal having a different optical density from the edges (**Figure 8(c)**). Both the spectra and the intensity map show that the centre of the crystal has lost almost all of its hydroxyl groups, while the hydroxyl group concentration around the edges of the crystal is less than 50% of that in the original calcined crystal before steaming (note the absorbance scale changes in the IR maps). Despite these changes in acid sites the crystallinity measured by XRD is unchanged.

The effects of these changes on the chemistry occurring when methanol is injected into the crystals was also investigated. As discussed above, surface methoxy groups are formed when methanol reacts with Brønsted acid hydroxyl groups in HSAPO-34 just as in H-ZSM-5. Following methoxy group formation there is a similar induction period before the first alkene products are formed, hydroxyl groups regenerated and methoxy groups converted to alkoxide species (21). The reduced hydroxyl group concentrations in steamed HSAPO-34 crystals also result in an increased induction period for hydroxyl group recovery and a much slower recovery, as shown in **Figure 9**. These differences are consistent with the increased average distance between methoxy groups slowing propagation of the carbon-carbon bond forming reactions through the crystal.

Injection of methanol at higher temperatures causes the immediate appearance of the IR signature of alkoxide groups formed from alkene oligomerisation. **Figure 10** compares the effects of injecting three successive pulses of methanol at 623 K into a fresh and steamed crystal of HSAPO-34 (note absorbance scale in **Figure 10(b)** is five-fold expanded). In the fresh crystal, dimethyl ether and propene are evolved after a very short induction period following the first methanol pulse and the IR spectrum shows the alkoxide ν(CH) bands. Injection of a second pulse hardly changes the IR spectrum and the dimethyl ether and propene yields are reduced, while the third pulse forms negligible amounts of dimethyl ether and propene. The loss of activity is not due to removal of acid sites but is caused by oligomer formation in the outer regions of the crystal blocking the pores.

In the steamed crystal dimethyl ether and propene formation continue after three pulses of methanol and the alkoxide ν(CH) bands continue to grow (note the IR spectra in **Figure 9(b)** have been scaled by a factor of five reflecting the fivefold reduction in hydroxyl concentration in the steamed crystal). Although these SAPO-34 crystals are much larger than those used in the commercial MTO process and deactivate much more quickly (21), the microspectroscopy experiments provide highly relevant insight into the beneficial effects of mild steaming i.e. reducing acid site density inhibits formation of pore blocking oligomers. This is consistent with the observed prolonged catalyst lifetime in laboratory fixed bed reactor tests of moderately steamed samples.

Catalytic Chemistry: Selective Catalytic Reduction of Nitric Oxide with Ammonia

We report here hitherto unpublished results of preliminary experiments using the *in situ* IR microspectroscopy approach to examine the reaction of nitric oxide with ammonia over single

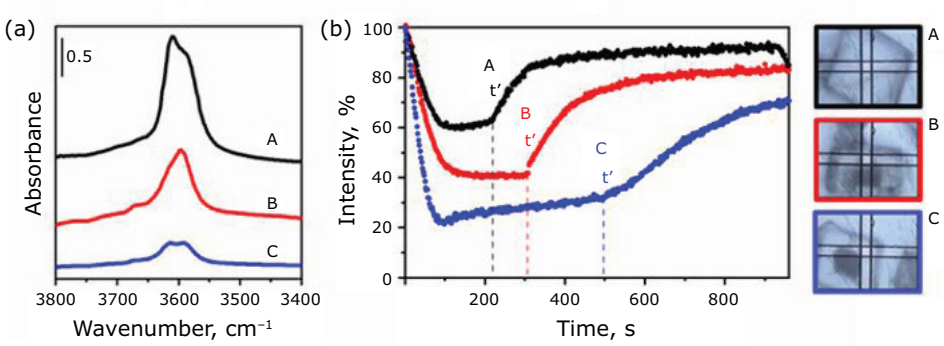

Fig. 9. (a) FTIR spectra of dehydrated: A = fresh HSAPO-34 (black); B = HSAPO-34 steamed 20 hours at 973 K (red); C = 44 hours at 973 K (blue); (b) time course of the ν(OH) intensity at 3600 cm^{-1} following injection of a single methanol pulse at 573 K expressed relative to that prior to methanol injection. Reprinted from (26) with permission from Elsevier

crystals of a CuSAPO-34 catalyst. Conventionally, copper zeolite catalysts for nitric oxide SCR are prepared by ion exchange, but in the case of SAPO-34 this can lead to a loss of crystallinity and an inhomogeneous distribution of Cu^{2+} cations. An alternative approach is to utilise copper-polyamine complexes as templates, which enables the direct inclusion of complexed Cu^{2+} cations in the solid. Calcination then releases the Cu^{2+} cations to extra-framework sites distributed uniformly throughout the crystals and removes the need for an ion exchange step (27).

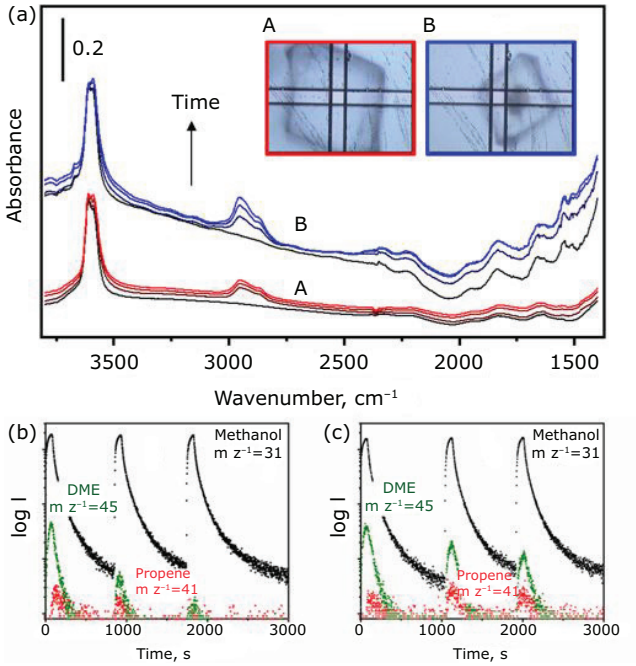

Fig. 10. (a) IR microspectra of: A = fresh HSAPO-34 crystal; B = H-SAPO-34 crystal steamed at 973 K 44 hours during exposure of 1, 2 and 3 pulses of methanol at 623 K. Growth of organic species adsorbed with each pulse are more notable on the edge of the steamed sample. Note five-fold expansion of absorbance scale of B; (b) MS analysis of A; (c) MS analysis of B. Reproduced from (26) with permission from Elsevier

Large (~50 μm) crystals of CuSAPO-34 were prepared by this method and shown to have good activity for nitric oxide SCR in laboratory microreactor tests (**Figure 11(a)**). The IR microspectrum of a single crystal of CuSAPO-34 after calcination is compared in **Figure 11(b)** with that of a similar sized crystal of HSAPO-34. The Cu^{2+} containing SAPO-34 still contains Brønsted acid sites (the ν(OH) bands around 3600 cm^{-1} with an additional ν(OH) band at 3535 cm^{-1} attributed to hydroxyl groups located in the smaller d6 ring of the H-SAPO-34 framework). The lower frequency bands at 2200–1400 cm^{-1} are due to the SAPO-34 framework.

We used the *in situ* reactor capability at MIRIAM to observe changes in the spectra of single crystals when a CuSAPO-34 crystal was first loaded with ammonia then the adsorbed ammonia reacted with nitric oxide (**Figure 12**).

Ammonia adsorption in HSAPO-34 (dotted trace in **Figure 12(a)**) forms NH_4^+ by reaction with the Brønsted acid sites. In CuSAPO-34, the same species are generated but additional bands characteristic of ammonia coordinated to Cu^{2+} grow (3332 cm^{-1}, 3185 cm^{-1} and 1620 cm^{-1}). All of the Brønsted acid sites are accessible to ammonia, as seen by the complete loss of the ν(OH) bands (compare the green trace to the orange trace of activated CuSAPO-34 in **Figure 12(a)**).

On subsequent introduction of nitric oxide (**Figure 12(b)**) the entire envelope of bands, due to the bound ammonia on acid sites and copper cations, reacts at the same observed rate. The initial rate at which the bound ammonia on the two distinct Brønsted acid sites reacted with the nitric oxide was slightly reduced for the acid site located in the smaller d6 rings (the 3635 cm^{-1} band).

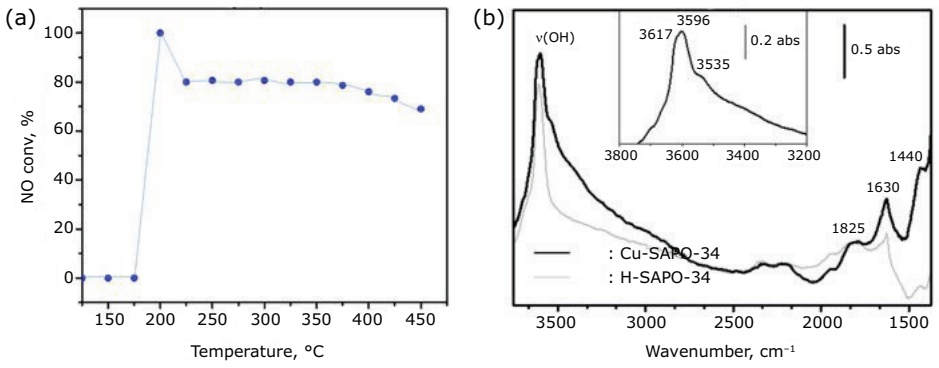

Fig. 11. (a) Nitric oxide conversion during microcatalytic testing of CuSAPO-34 crystals under standard ammonia-SCR conditions (15 ml min^{-1} 1% nitric oxide, 3 ml min^{-1} 5% ammonia, 30 ml min^{-1} 20% oxygen); (b) IR microspectra of dehydrated single crystals of SAPO-34 (grey trace) and CuSAPO-34 (black trace)

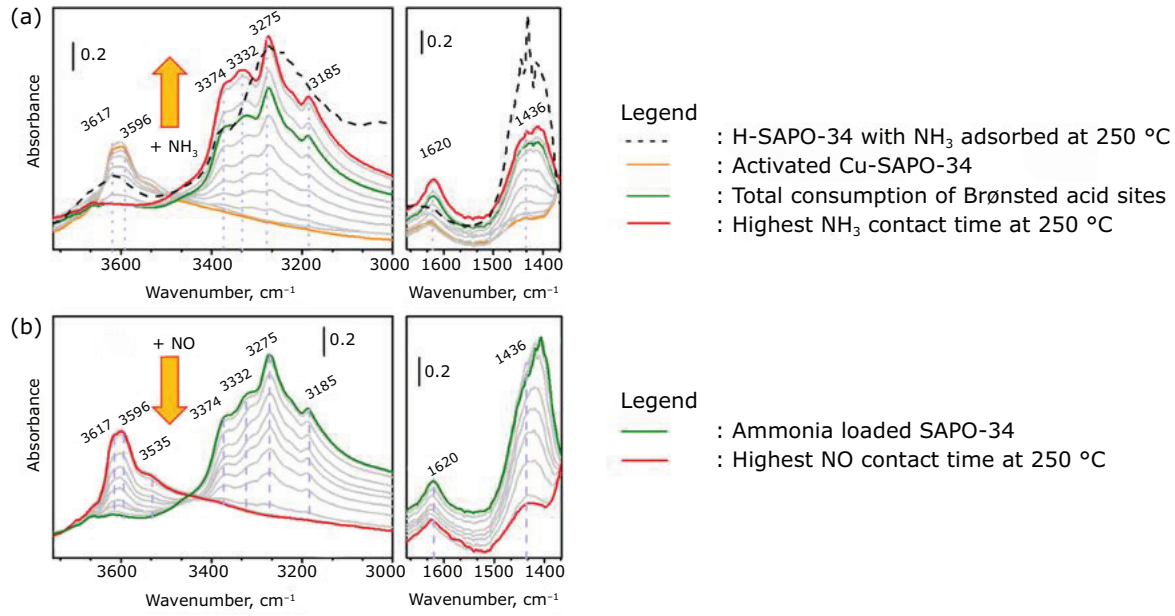

Fig. 12. (a) IR microspectra showing the progressive loss of Brønsted acid hydroxide groups and growth of adsorbed ammonia bands on a single crystal of CuSAPO-34 exposed to ammonia at 523 K. Overlayed dotted trace of the dehydrated single crystals of HSAPO-34; (b) progressive loss of adsorbed ammonia and recovery of Brønsted acid sites when the ammonia loaded CuSAPO-34 crystal is exposed to nitric oxide at 523 K. The highest contact time in both graphs is shown after 20 min (red spectra)

High quality time-resolved FTIR microspectra follow the build-up of bound ammonia on both acid sites and copper cations over the homogeneous large CuSAPO-34 single crystals used to study the selective catalytic reduction of nitric oxide with ammonia. More work is needed to investigate reaction mechanisms in detail, but these preliminary observations clearly show the capability of such *operando* microspectroscopy FTIR measurements for reactive catalytic chemistry.

Future Prospects

The examples described above illustrate how IR microspectroscopy coupled to synchrotron radiation can be used for *in situ* catalytic studies on zeolite single crystals. The crystals studied *in situ/operando* are of necessity larger than those found in industrial catalysis, but for model studies of reaction mechanisms in particular the method is proven to be extremely powerful. There are a number of ways in which the technology can be improved which will further expand the scope of the method. Optimum spatial resolution and signal to noise ratio both call for the highest possible magnification objective in the microscope. This however reduces substantially the working depth available to accommodate a sample cell. Modification of the commercial Linkam cell allowed use of a 36× magnification objective for some of the work described above, but this also revealed some other limitations of the commercial cell which the MIRIAM beam line team and engineers at Diamond Light Source have overcome by designing in house a specialised reaction cell which accommodates the 36× objective.

The new cell has another two important advantages: the dead volume of the cell is reduced, allowing much faster reaction analysis, and all of the internal surfaces of the sample volume are heated, unlike the cooled internal surfaces of the Linkam cell which may retain adsorbed water or other reactants. The first prototype of the new cell which we have recently tested has an internal volume of <1 ml compared with ~100 ml for the Linkam cell.

An issue with commercial *in situ* cells is the possibility of working with toxic or highly flammable reactive gases and the risk of leakage from the cell. The new B22 design overcomes this risk by enclosing the cell in an outer jacket which is continuously flushed with nitrogen. **Figure 13** is a photograph of the prototype cell showing the inner reaction cell with zinc selenide windows inside the outer jacket (which has had the upper window removed to show the interior). Within the inner cell, the zeolite crystals are placed on the

Fig. 13. Photograph of prototype *in situ* reaction cell used in the IR microscope in 2023 (window of the outer jacket removed). The inner heated cell contains zeolite crystals on a zinc selenide window

zinc selenide lower window of the cell and the cell sealed by attaching an upper window. This cell has been tested by studying the oligomerisation of olefins in H-ZSM-5 crystals at temperatures up to 523 K (the present upper limit of the O-ring seals). A full description of the cell will be presented in a future publication (28).

Another issue with the Linkam cell which the new Diamond Light Source prototype does not yet fully overcome is temperature stability of the sample position. Ideally, temperature programmed reaction studies involve measuring spectra from one particular position in a crystal as the temperature is ramped upwards in flowing reactant gases. In practice, micrometre-scale movements of the crystal as the temperature is changed require manual intervention to maintain the same focus position. Future solutions to this problem may involve upgrades to the cell design or software-based approaches using the motorised microscope sample stage to track the sample position during temperature ramps.

Other future goals at the MIRIAM beamline are automated IR microspectroscopy of multiple crystals in the same loading for better statistics at single crystal level, for high throughput and lesser artefact (sample loading and reloading issues and or reproducibility) and development of software to speed up the processing and analysis of the very large data sets which the technique can generate.

Finally, we mention new IR methods which can overcome the diffraction limit restricting the spatial resolution in optical IR microscope, i.e. how to go into the submicron scale. This is IR nanospectroscopy, for which there are several technical variations that use an atomic force microscope (AFM) to detect the sample absorption illuminated by an IR microbeam, in the B22 case originating from Diamond Light Source. Since no optics define the measured signal, spatial resolution is dictated by the actual AFM tip, typically 10–100 nm wide. Near-field IR spectroscopy can either probe: (i) the thermomechanical local expansion following sample temperature rise resulting from its IR absorption and revealed by the AFM tip cantilever amplitude resonance (known as the photothermal in resonance method or AFM-IR); or (ii) the phase change due to the interaction between the oscillating cantilever tip and the sample over an IR reflective substrate when the sample absorption modifies the local 'antenna effect' with the IR microbeam shone at grazing angle: scattering-type scanning near-field optical microscopy (s-SNOM). Both of these methods are now uniquely available at the MIRIAM beamline B22 at Diamond. In the literature s-SNOM and AFM-IR have been applied to obtain IR spectra of MOF zeolites (29) and ZSM-5 zeolite films comprising crystals ~1 μm in size (30), respectively. However, adapting these AFM based methods for *in situ operando* spectroscopy of small crystals of zeolite catalysts remains a scientific challenge to be addressed with an *ad hoc* example miniature sample environment still to be devised. In the longer term, such methods offer the possibility of *operando* microspectroscopy on zeolite crystals of industrial sizes (~1 μm).

Acknowledgements

The research leading to these results has received primary funding from the Engineering and Physical Sciences Research Council Centre for Doctoral Training in Critical Resource Catalysis (EP/IO17008/1 and supplementary equipment Grant EP/L016419/1). ScotCHEM, the Society of Chemical Industry and Santander - St Leonard's College are thanked for the scholarships provided during Ivalina's PhD. The Diamond Light Source is thanked for provision of beam time and support

facilities at the MIRIAM beamline B22 (experiments SM13725-1, SM14114-1, SM16257-1, SM18680-1, SM20906-1, SM23471-1 and SM23471-2 and SM23808-1). Johnson Matthey is thanked for their in-kind contributions and support during the steaming study. The Catalysis Hub is thanked for their support during the microcatalytic testing of Cu-SAPO-34 crystals under standard ammonia selective catalytic reduction conditions. Publications arising from this research are cited throughout this article.

References

1. S. Bordiga, C. Lamberti, F. Bonino, A. Travert, F. Thibault-Starzyk, *Chem. Soc. Rev.*, 2015, **44**, (20), 7262
2. F. Zaera, *J. Catal.*, 2021, **404**, 900
3. F. C. Meunier, *React. Chem. Eng.*, 2016, **1**, (2), 134
4. A. Vimont, F. Thibault-Starzyk, M. Daturi, *Chem. Soc. Rev.*, 2010, **39**, (12), 4928
5. J. J. Bravo-Suárez, P. D. Srinivasan, *Catal. Rev.*, 2017, **59**, (4), 295
6. M. Nowotny, J. A. Lercher, H. Kessler, *Zeolites*, 1991, **11**, (5), 454
7. F. Schueth, *J. Phys. Chem.*, 1992, **96**, (19), 7493
8. F. Schueth, D. Demuth, B. Zibrowius, J. Kornatowski, G. Finger, *J. Am. Chem. Soc.*, 1994, **116**, (3), 1090
9. F. Marlow, D. Demuth, G. Stucky, F. Schueth, *J. Phys. Chem.*, 1995, **99**, (4), 1306
10. S. C. Popescu, S. Thomson, R. F. Howe, *Phys. Chem. Chem. Phys.*, 2001, **3**, (1), 111
11. E. R. Geus, J. C. Jansen, H. van Bekkum, *Zeolites*, 1994, **14**, (2), 82
12. E. Stavitski, M. H. F. Kox, I. Swart, F. M. F. de Groot, B. M. Weckhuysen, *Angew. Chem. Int. Ed.*, 2008, **47**, (19), 3543
13. M. H. F. Kox, K. F. Domke, J. P. R. Day, G. Rago, E. Stavitski, M. Bonn, B. M. Weckhuysen, *Angew. Chem. Int. Ed.*, 2009, **48**, (47), 8990
14. Q. Qian, J. Ruiz-Martínez, M. Mokhtar, A. M. Asiri, S. A. Al-Thabaiti, S. N. Basahel, H. E. van der Bij, J. Kornatowski, B. M. Weckhuysen, *Chem. Eur. J.*, 2013, **19**, (34), 11204
15. Q. Qian, J. Ruiz-Martínez, M. Mokhtar, A. M. Asiri, S. A. Al-Thabaiti, S. N. Basahel, B. M. Weckhuysen, *ChemCatChem*, 2014, **6**, (3), 772
16. G. Cinque, M. Frogley, K. Wehbe, J. Filik, J. Pijanka, *Synchrotron Radiat. News*, 2011, **24**, (5), 24
17. A. Zecchina, F. Geobaldo, G. Spoto, S. Bordiga, G. Ricchiardi, R. Buzzoni, G. Petrini, *J. Phys. Chem.*, 1996, **100**, (41), 16584
18. I. B. Minova, S. K. Matam, A. Greenaway, C. R. A. Catlow, M. D. Frogley, G. Cinque, P. A. Wright, R. F. Howe, *Phys. Chem. Chem. Phys.*, 2020, **22**, (34), 18849
19. Z. Ristanović, J. P. Hofmann, U. Deka, T. U. Schülli, M. Rohnke, A. M. Beale, B. M. Weckhuysen, *Angew. Chem. Int. Ed.*, 2013, **52**, (50), 13382
20. I. B. Minova, S. K. Matam, A. Greenaway, C. R. A. Catlow, M. D. Frogley, G. Cinque, P. A. Wright, R. F. Howe, *ACS Catal.*, 2019, **9**, (7), 6564
21. I. B. Minova, M. Bühl, S. K. Matam, C. R. A. Catlow, M. D. Frogley, G. Cinque, P. A. Wright, R. F. Howe, *Catal. Sci. Technol.*, 2022, **12**, (7), 2289
22. I. Yarulina, A. D. Chowdhury, F. Meirer, B. M. Weckhuysen, J. Gascon, *Nat. Catal.*, 2018, **1**, (6), 398
23. W. Song, Y. Wei, Z. Liu, 'Chemistry of the Methanol to Olefin Conversion', in "Zeolites in Sustainable Chemistry: Synthesis, Characterization and Catalytic Applications", eds. F.-S. Xiao, X. Meng, Green Chemistry and Sustainable Technology Series, Springer-Verlag, Berlin, Germany, 2016, pp. 299–346
24. W. Dai, G. Wu, L. Li, N. Guan, M. Hunger, *ACS Catal.*, 2013, **3**, (4), 588
25. J. Zhou, J. Zhang, Y. Zhi, J. Zhao, T. Zhang, M. Ye, Z. Liu, *Ind. Eng. Chem. Res.*, 2018, **57**, (51), 17338
26. I. B. Minova, N. S. Barrow, A. C. Sauerwein, A. B. Naden, D. B. Cordes, A. M. Z. Slawin, S. J. Schuyten, P. A. Wright, *J. Catal.*, 2021, **395**, 425
27. A. Turrina, E. C. V. Eschenroeder, B. E. Bode, J. E. Collier, D. C. Apperley, P. A. Cox, J. L. Casci, P. A. Wright, *Microporous Mesoporous Mater.*, 2015, **215**, 154
28. M. D. Frogley, G. Cinque, *in preparation*
29. A. F. Möslein, J.-C. Tan, *J. Phys. Chem. Lett.*, 2022, **13**, (12), 2838
30. D. Fu, K. Park, G. Delen, Ö. Attila, F. Meirer, D. Nowak, S. Park, J. E. Schmidt, B. M. Weckhuysen, *Chem. Commun.*, 2017, **53**, (97), 13012

The Authors

Russell Howe is an Emeritus Professor of Materials Chemistry at the University of Aberdeen. Following education in New Zealand he pursued postdoctoral studies at Edinburgh University, Texas A&M and CSIRO Australia before taking academic positions at the University of Wisconsin-Milwaukee, University of Auckland, University of New South Wales and University of Aberdeen (since 2001). His interests are in applications of spectroscopy to study materials, surfaces and catalysts.

Paul Wright has been on the Chemistry staff at St Andrews since 1994 and Full Professor since 2010. He completed his PhD in Physical Chemistry with Sir John Meurig Thomas at Cambridge and worked with him at the Royal Institution in London as Assistant Director before moving to St Andrews. His research focuses on the synthesis and structural elucidation of porous solids, including new zeolites and MOFs and their applications in catalysis, gas separation and carbon capture. This requires advanced characterisation by *in situ* diffraction and spectroscopy, combined with measurements of adsorption and catalytic performance and supported by molecular modelling. He has published over 200 research articles, several patents and a Royal Society of Chemistry (RSC) monograph. He has increasingly collaborated with industry and he is currently a Royal Society Industrial Fellow with Johnson Matthey.

Ivalina Tuxworth obtained a PhD from the University of St Andrews in 2020, for which she received the RSC best PhD thesis award in the area of surface reactivity and catalysis. She is an author of four journal articles and a book chapter. She started her career at Johnson Matthey as a Research Scientist. Since 2021, Ivalina is training scientists to use new science software and equipping them with modern digitalisation and data stewardship tools to capture research and development data.

Mark D. Frogley is Senior Beamline Scientist at the MIRIAM IR beamline (B22) at Diamond Light Source synchrotron, UK. His interests are in optical spectroscopy technique and instrument development, as well as applications focused on porous materials. He obtained his PhD in semiconductor physics at Queen Mary and Westfield College, University of London in 2000 and continued his academic research at the Weizmann Institute of Science and Imperial College London before joining Diamond in 2007.

Gianfelice Cinque is the Principal Scientist for the IR beamline (MIRIAM) at Diamond Light Source since 2006. He is visiting fellow at the Department of Engineering Sciences at the University of Oxford since 2021. His scientific interests range from the multidisciplinary use of synchrotron IR radiation, including terahertz microscopy for example on MOF and composite materials, to biomedical studies at subcellular level *via* IR nanospectroscopy and IR imaging *ex vivo/in vitro* at high magnification, also *via* adaptive optics. He graduated in Physics at Padua University, Italy, and obtained a PhD in General Physics at Ferrara University, Italy, working also at CERN, Geneva, Switzerland. He joined Diamond from the INFN laboratories of Frascati, Italy, where he was mainly responsible for the soft X-ray beamline and was previously a scientist on the IR beamline.